Journal of
Materials Chemistry B

RSC Publishing

PAPER

View Article Online
View Journal | View Issue

Cite this: *J. Mater. Chem. B*, 2013, **1**, 835

Ionically interacting nanoclay and nanofibrillated cellulose lead to tough bulk nanocomposites in compression by forced self-assembly

Hua Jin,*[a] Anyuan Cao,[b] Enzheng Shi,[b] Jani Seitsonen,[c] Luhui Zhang,[b] Robin H. A. Ras,[a] Lars A. Berglund,[d] Mikael Ankerfors,[e] Andreas Walther[f] and Olli Ikkala*[a]

Received 5th November 2012
Accepted 12th November 2012

DOI: 10.1039/c2tb00370h

www.rsc.org/MaterialsB

Several approaches have recently been shown for self-assembled biomimetic composite films, aiming at combinations of high toughness, strength, and stiffness. However, it remains challenging to achieve high toughness using simple processes especially for bulk materials. We demonstrate that ionically interacting cationic native nanofibrillated cellulose (C-NFC) and anionic nanoclay, *i.e.* montmorillonite (MTM), allow local self-assemblies by a simple centrifugation process to achieve 3D bulk materials. The composite with MTM/C-NFC of 63/37 w/w has a high compressive strain to failure of 37% with distinct plastic deformation behaviour, a high work to fracture of 23.1 MJ m^{-3}, and a relatively high compression strength of 76 MPa. Unlike the conventionally used sequential deposition methods to achieve well-defined layers for the oppositely charged units as limited to films, the present one-step method allows quick formation of bulk materials and leads to local self-assemblies, however, having a considerable amount of nanovoids and defects between them. We suggest that the nanovoids and defects promote the plastic deformation and toughness. Considering the simple preparation method and bio-based origin of NFC, we expect that the present tough bulk nanocomposites in compression have potential in applications for sustainable and environmentally friendly materials in construction and transportation.

Introduction

Materials with high toughness, stiffness, strength, and low density are of great interest in load-bearing applications, *e.g.* in construction and transportation, if they are processable, scalable, and economic. This synergistic combination of properties can potentially be achieved by composite nanostructure concepts, but has so far been difficult to achieve.[1] However, nature shows a wide variety of tough lightweight nanocomposite materials having combinations of excellent mechanical properties, where nacre and bone are classical examples.[2–9] They are not technologically feasible due to the complexity of biological systems but suggest routes for biomimetic materials science.[10–15] In tough biocomposites, there is a common design principle consisting of hierarchical self-assemblies of high weight fraction of aligned inorganic or organic reinforcing nanoscale domains promoting stiffness, and soft organic domains enable fracture energy dissipation to suppress catastrophic crack propagation in deformation.[2] The soft domains contribute to a complex combination of mechanisms, *e.g.*, interdomain slippages and reinforcement pull-out, weak links, sacrificial bonds, deformation of macromolecular conformations, and hidden length scales.[3,6–8] Nacre is comprised of more than 90% of inorganic aragonite platelets separated by thin layers of organic matter. Its toughness is about three orders of magnitude higher than that of pure aragonite.[2] Bone has a more complex hierarchical structure, in which there is *ca.* 65% hydroxyapatite with 25% collagen fibrils and 10% water.[2] However, the fraction of different components varies depending on the species of bone.

Even if understanding the toughening mechanisms of biomatter is a considerable scientific challenge as such,[3–8] the already elucidated features suggest routes for man-made biomimetic tough materials. Since the biological materials cannot be scaled for technologies due to their complicated biosynthesis, a range of biomimetic materials have been demonstrated incorporating the above mentioned biological concepts: at the simplest level, *e.g.* nacre-mimetic composites

[a]*Department of Applied Physics, Aalto University (formerly Helsinki University of Technology), P.O. Box 15100, FI-02150 Espoo, Finland. E-mail: olli.ikkala@aalto.fi; hua.jin@aalto.fi; Fax: +358-9-470 23155; Tel: +358-9-47001*

[b]*College of Engineering, Department of Advanced Materials and Nanotechnology, Peking University, Beijing 100871, P.R. China*

[c]*Nanomicroscopy Centre, Aalto University, P.O. Box 15100, FI-02150 Espoo, Finland*

[d]*Wallenberg Wood Science Centre & Department of Fibre and Polymer Technology, KTH, Royal Institute of Technology, SE-100 44 Stockholm, Sweden*

[e]*Innventia AB, SE-11486 Stockholm, Sweden*

[f]*DWI at RWTH Aachen University, 52056 Aachen, Germany*

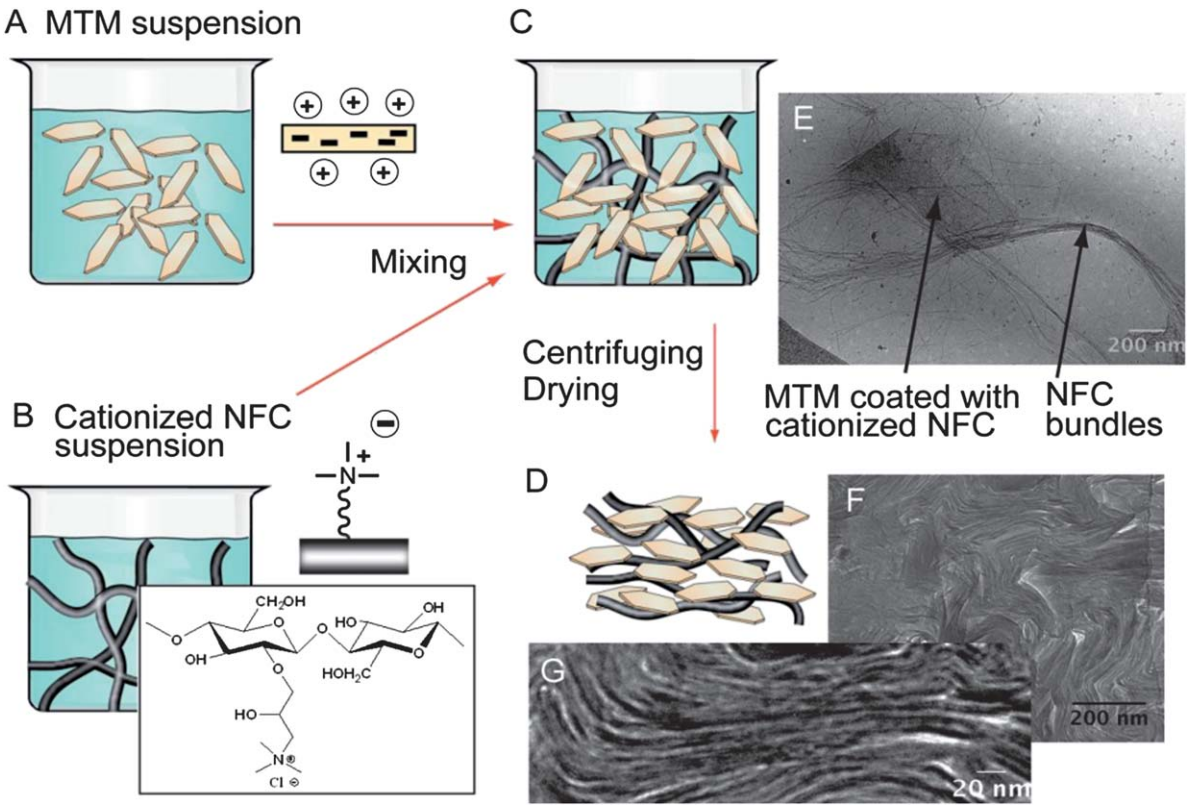

Fig. 1 Scheme of the process to prepare tough biocomposites from cationic nanofibrillated cellulose (C-NFC) and montmorillonite (MTM). (A) 2 wt% suspension of MTM. (B) 0.23 wt% hydrogel of C-NFC with surface groups of *N*-(2,3-epoxypropyl)trimethylammonium. (C) The aqueous MTM and C-NFC suspensions mixed. (D) Composite material after forced packing by centrifugation and drying. (E) Cryo-TEM image for the case (C) showing that the MTM platelets are coated with C-NFC. (F) Cross-sectional TEM image of (D) showing local self-assembled domains with no overall common alignment. (G) Higher magnification TEM shows one self-assembled domain with nanovoids or defects.

could be constructed by applying alternating layers of inorganic reinforcing nanosheets and soft energy dissipating polymeric layers. Several approaches have been provided based on layer-by-layer deposition, sequential spin coatings, ice-templating and sintering, and self-assembly of polymer-coated reinforcing nano-objects.[10–15] Faithful mimicking of bone is more challenging due to its hierarchical structure, but toughness of bone from a combination of collagen fibrils and hydroxyapatite[3,6–8] may suggest incorporation of mutually interacting deformable nanofibrils with mineral nanoplatelets.

Here we ask whether concepts and compositions for promoted toughness under compression in 3D, *i.e.*, bulk specimen can be achieved by incorporating some of the above-mentioned biomimetic principles. We explore particularly simple ways by self-assembling ionically interacting cationic native cellulose nanofibrils (C-NFCs) and negatively charged inorganic nanoplatelets, *i.e.*, montmorillonite (MTM) to form bio-based tough bulk nanocomposites using a one-step process. In particular, we aim to avoid the sequential polyelectrolyte deposition processes[16] which are classically used to assemble the oppositely charged units to form ordered films and which are not scalable for bulk specimens. Native nanocelluloses have recently become topical as they have extraordinary mechanical properties due to their native crystalline structures, as derived from the high axial crystal modulus of cellulose I of *ca.* 140 GPa, and due to their sustainability, large scale availability, and feasible preparation techniques.[17–23] Native nanocelluloses can be cleaved from wood or plant cell walls to form hydrogels, importantly avoiding a complete dissolution into molecular cellulose chains, and have diameters in the range of ten nanometres or less. Two main classes exist: short rod-like nanocrystals and long, coiled and entangled nanofibrillated cellulose (NFC), also denoted as microfibrillated cellulose.[17–19]

NFC allows the preparation of various functional materials and composites.[24–40] Here we use NFC, as the high aspect ratio was expected to promote the mechanical properties as suggested by the long collagen fibres in bone. So far, MTM has extensively been used in conventional nanocomposites by mixing them into a polymer matrix.[1,41–43] Recently, hybrid nanopapers of MTM with slightly anionically charged NFC were prepared by filtration, which, however, did not show high toughness or reinforcement effects obviously due to poor interaction between MTM and NFC.[33,34] This encouraged us to incorporate ionic interaction in this work. Cationic NFC has also been shown to allow exfoliation of MTM.[40] Here we show that simple centrifugation processes allow bulk (3D) composites of C-NFC/MTM with local domains of self-assemblies, and specific tough compositions are identified with high strain to failure, compressive strength, high work to fracture, and low density.

Results and discussion

Fig. 1 shows a scheme for the preparation. Firstly, C-NFC and MTM were separately dispersed in water (see Methods), which led to essentially clear suspensions. Thereafter the two dispersions were mixed at relative weight fractions MTM/C-NFC 91/9, 81/19, 63/37, and 50/50 w/w. We selected a high weight fraction of the inorganic component owing to biomimetic design principles suggesting high levels of reinforcement. The resulting mixtures showed increased turbidity (Fig. 2B) due to the formation of large colloidal complexes as the oppositely charged C-NFC can bridge several MTM nanoplatelets to form ionically bound networks. Fig. 1E shows a MTM platelet having lateral dimensions of *ca.* 300 nm as covered by C-NFC fibrils and two C-NFC bundles. Typically, floc-like aggregates would be regarded to be detrimental to achieve well-defined self-assemblies and long-range order in the final compositions due to packing frustrations caused by aggregates. But interestingly, upon forced packing by centrifugation followed by drying, one obtains local self-assemblies, shown in Fig. 1G for the MTM/C-NFC 63/37 w/w. Even if Fig. 1G shows domains of locally aligned self-assemblies, the periodicity is not exactly defined, being in the range of 5–10 nm. C-NFCs have diameters in the same range as deduced from the cryo-TEM image in Fig. 1E. Note that a single exfoliated MTM has a thickness of *ca.* 1 nm.[10,14] A loose intercalation of the C-NFC leads to nanovoids between the nanoplatelets and defect domains are observed between the self-assembled domains. Fig. 1F shows the structure at a larger length scale for MTM/C-NFC 63/37 w/w: in the range of tens of nm, layered domains are observed, while in the range of hundreds of nm, the structure becomes anisotropic, as there is no coordinated alignment between the domains. The density of MTM/C-NFC 63/37 w/w is 2.17 g cm^{-3}. This suggests an overall porosity in the range of 4%, taken the nominal densities of C-NFC of 1.5 g cm^{-3} and MTM of 2.7 g cm^{-3}. Note that the dense set of defects and porosity may play an important role in the pronounced toughness, as it has been shown that a dense set of defects can provide deflected pathways for crack propagation in model systems.[5]

Compressive stress–strain measurements are shown in Fig. 2A. The composition with MTM/C-NFC of 91/9 w/w shows relatively low strain to failure and strength compared to others in this work. It demonstrates catastrophic failure in a brittle manner as the material totally disintegrates into small pieces under compression as shown in Fig. 3C. However, when more C-NFC is added to the composite, strain to failure and strength are increased substantially in a synergistic manner. For the sample with MTM/C-NFC of 81/19 w/w, the stress–strain curve shows a plateau for strain >10%, indicating the onset of plastic deformation. Table 1 summarizes the mechanical properties of the nanocomposites with different compositions. The best mechanical properties were observed for MTM/C-NFC with 63/37 w/w where the strain to failure is very high, close to 37% and the strength and modulus are 75.6 MPa and 512 MPa respectively. The area below the stress–strain curve, *i.e.* work to fracture, gives a qualitative measure of the toughness, and in the present case, it is as high as 23.1 MJ m^{-3}. Finally, increasing the weight fraction of C-NFC for MTM/C-NFC 50/50 w/w leads to decreased mechanical properties, indicating the composition 63/37 w/w is close to optimal.

We suggest that at high weight fractions of MTM there exists an insufficient amount of C-NFC to bridge the MTM platelets by their ionic interactions. Therefore such compositions are weak and brittle. On the other hand, at too high a fraction of C-NFC, there is an insufficient amount of reinforcing MTM. Between these opposite regimes there exists a synergistic composition, combining high strain and relatively high strength.

In comparison to other bio-based materials, the compressive mechanical properties regarding strain, strength, and stiffness in this work are comparable to the composites from clay and soybean, whereas higher values are reported for some composites using engineering polymers.[43,44] The present work

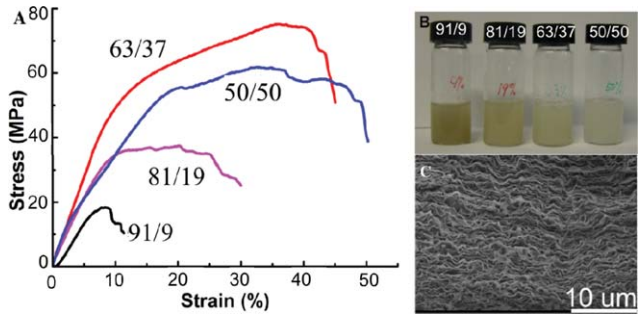

Fig. 2 (A) Compressive stress–strain curves for the MTM/C-NFC of 91/9, 81/19, 63/37, 50/50 w/w. Except for the first one, all of the compositions show distinct plastic deformation. The composition 63/37 w/w shows the best performance and is described more closely. (B) The aqueous C-NFC and MTM suspensions become turbid upon mixing, indicating aggregate formation. (C) SEM image of composite MTM/C-NFC of 63/37 w/w, indicating "wavyness" of the assembly, which may also promote toughness.

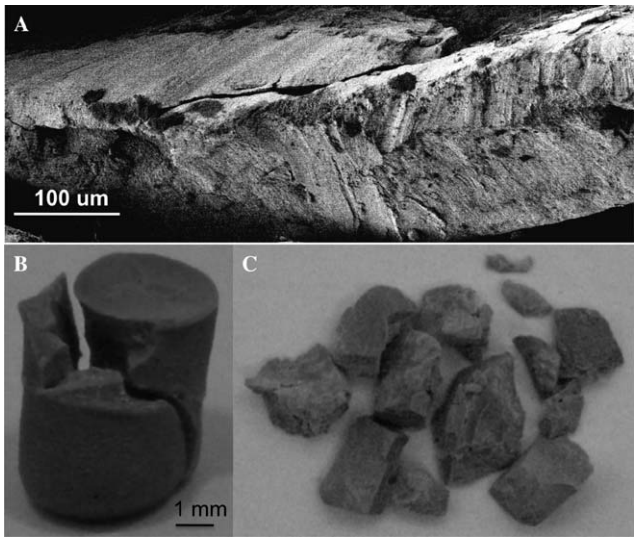

Fig. 3 Examples of fractures. (A) Cross-sectional SEM image of cracks from the composite with MTM/C-NFC of 63/37 w/w showing rough crack surfaces. (B) MTM/C-NFC 63/37 w/w after compression failure, showing deflected crack path. (C) Photo of pieces from a composite with MTM/C-NFC of 91/9 w/w after compression failure, indicating brittleness.

Table 1 Summary of compressive mechanical properties of the nanocomposites with different compositions

Composite MTM/C-NFC	Compressive strength (MPa)	Modulus (MPa)	Work to fracture (MJ m^{-3})
91/9 w/w	22.3 ± 4.8	339 ± 25	2.49 ± 0.7
81/19 w/w	38.7 ± 12.5	454 ± 35	12.3 ± 0.1
63/37 w/w	75.6 ± 1.6	512 ± 94	23.1 ± 5.4
50/50 w/w	64.2 ± 7.7	379 ± 40	22.7 ± 2.0

to fracture of 23.1 MJ m^{-3} is surprisingly high due to the contribution of a high strain to failure of 37%. The biological material abalone shows in compression a strain to failure of 0.6% without significant plastic deformation, but a very high strength of 380 MPa and a modulus of 34 GPa. Cortical bone shows a strain of 1.6% with plastic deformation in compression, a strength of 260 MPa, and a modulus of 25 GPa.[40] Compared to bone and nacre, further optimization needs to be done to improve the strength and stiffness of the composites achieved in this work. Regarding biomimetic inorganic–organic nanocomposites, the ice-templated, sintered, and polymerized Al_2O_3–polymethyl methacrylate hybrid showed a strain of 1.4%, a strength of 152 MPa, and a modulus of 40 GPa in bending, and a pronounced plastic deformation.[12] In tensile mode the sequentially deposited Al_2O_3–chitosan assembly showed a particularly high strain of 25%, a strength of 300 MPa, and a modulus of 7 GPa, with a highly pronounced plastic zone.[13] However, due to the different deformation modes, a direct quantitative comparison cannot be made for such cases.

Evidence of the toughness is given also upon studying the fracture of the sample with MTM/C-NFC of 63/37 w/w, see Fig. 3A and B. The cracks propagate in a deflected and tortuous way. Finding molecular and structural level origins for the high toughness is a challenging task, probably requiring multi-scale modelling in combination with extensive fracture analysis with *in situ* observations.[3,5] This is however beyond the scope of this work, at this point we can only give hypotheses for the high toughness. We expect that the ionic interaction between the MTM and cationized nanocellulose are relevant, akin to the ionic interactions between minerals and collagen fibres in bone.[3,8]

Cyclic compression results for the synergistic composition of 63/37 w/w are shown in Fig. 4. A relatively low strain of 5% is applied, which is much less than the maximum strain of nearly an order of magnitude larger. The figure demonstrates the hysteresis during cyclic loading, which is a manifestation of the energy dissipation.[40] It can be seen that in the first cycle, there is a 0.8% permanent residual strain in the material. The inset shows the development under consecutive loadings and unloadings. This also indirectly indicates the resilient mechanical properties of this composite material.

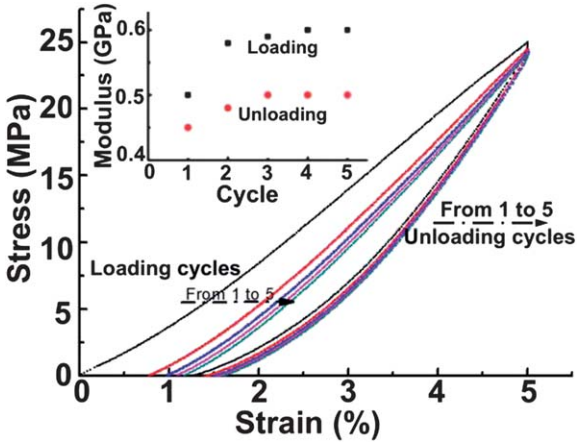

Fig. 4 Cyclic compressive mechanical properties of the composite with MTM/C-NFC of 63/37 w/w for 5 cycles using a strain of 5%. The inset shows the development of the modulus under consecutive loadings and unloadings.

Conclusions

In summary, in this work, a facile one-step route for a bulk 3D composite material with particularly high compressive strain to failure, distinct plastic deformation and high toughness was demonstrated from forced assembly of cationic cellulose nanofibrils and anionic nanoclay by centrifugation. This is encouraging, since the realization of load-bearing tough structural nanocomposites in bulk form is an important challenge in materials science. The optimal composition MTM/C-NFC of 63/37 w/w showed a high strain to failure of 37%, a strength of 76 MPa, and a high work to fracture of 23.1 MJ m^{-3} under compression. Considering the simple preparation methods, potentially low cost, and bio-based origin of C-NFC, the composites have potentials for applications in construction and transportation.

Methods

The C-NFC was supplied by Innventia AB (Sweden). It is a semi-transparent hydrogel with *N*-(2,3-epoxypropyl)trimethylammonium functionalities on the surface. The degree of substitution is 0.089, *i.e.* the total charge is 509.2 microeq. per g. Its aqueous suspension of concentration 0.23 wt% was used in this work. NFC fibrils have diameters in the range of 5–10 nm, their length is in the range of micrometers, and they form entangled networks.[21] MTM is an aluminosilicate clay named Bentonite from Sigma-Aldrich (CAS 1302-78-9 from Batch 067K0043). The platelets have a lateral dimension up to 1 μm and MTM nanoplatelets are known to have a thickness of *ca.* 1 nm.[13,40] A 2 wt% MTM suspension in water was prepared and mixed by magnetic stirring at 400 rpm for 24 h. C-NFC hydrogel was added to MTM suspension drop by drop to obtain MTM/C-NFC ratios of 91/9, 81/19, 63/37, and 50/50 w/w. The colloidal mixture of MTM and C-NFC was then mixed by an Ultraturrax mixer at 10 000 rpm for 1–2 min. The suspension with MTM and NFC was transferred to a 5 ml centrifugation tube. Centrifugation was done at 4000 rpm for 5 min. In order to obtain sufficiently thick 3D samples, a further amount of suspension of the mixture was added to the centrifugation tube after removing water on top. This was repeated 2 or 3 times. Thereafter the samples were dried at 60 °C for 2 days.

SEM images were taken using Hitachi S 4800 and JEOL (JSM 7500 A) field emission microscopes. A thin layer of Au was sputtered onto the samples before imaging. TEM images were obtained by a JEOL JEM-3200FSC cryo-TEM. Ultrathin sections were microtomed using a LEICA 125 Ultracut. Mechanical tests were carried out by Instron 5843 with 1 kN load cells using a strain rate of 1 mm min^{-1}. At least 5 samples were tested in compression for each composition. The variations are shown in Table 1. The average results in the table were based on at least 3 samples. The composition MTM/C-NFC of 63/37 w/w was characterized in more depth due to its close to optimal properties. During the cyclic compression test, it was compressed 5 times with a setting strain of 5%. Humidity during mechanical measurement was 20–31% as an average from the measurement room. The density of the sample with a composition of MTM/C-NFC of 63/37 w/w was 2.17 g cm^{-3}.

Acknowledgements

The work is funded by Academy of Finland, ERC, and EU FP7 SustainComp. Discussions with Tom Lindström, Lars Wågberg, Gero Decher, and Janne Laine are appreciated on various aspects on compositions. This work made use of the Aalto University Nanomicroscopy Centre facilities.

Notes and references

1 *Nanocomposite Science and Technology*, ed. P. M. Ajayan, L. S. Schadler and P. V. Braun, VCH-Wiley, Weinheim, 2004.
2 M. A. Meyers, P.-Y. Chen, A. Y.-M. Lin and Y. Seki, *Prog. Mater. Sci.*, 2008, **53**, 1–206.
3 M. E. Launey, M. J. Buehler and R. O. Ritchie, *Annu. Rev. Mater. Res.*, 2010, **40**, 25–53.
4 J. W. C. Dunlop and P. Fratzl, *Annu. Rev. Mater. Res.*, 2010, **40**, 1–24.
5 D. Sen and M. J. Buehler, *Sci. Rep.*, 2011, 1.
6 H. Peterlink, P. Roschger, K. Klaushofer and P. Fratzl, *Nat. Mater.*, 2006, **5**, 52–55.
7 C. Mercer, M. Y. He, R. Wang and A. G. Evans, *Acta Biomater.*, 2006, **2**, 59–68.
8 M. J. Buehler, *Proc. Natl. Acad. Sci. U. S. A.*, 2006, **103**, 12285–12290.
9 R. Z. Wang and H. S. Gupta, *Annu. Rev. Mater. Res.*, 2011, **41**, 41–73.
10 Z. Tang, N. A. Kotov, S. Magonov and B. Ozturk, *Nat. Mater.*, 2003, **2**, 413–418.
11 S. Deville, E. Saiz, R. K. Nalla and A. P. Tomsia, *Science*, 2006, **311**, 515–518.
12 E. Munch, M. E. Launey, D. H. Alsem, E. Saiz, A. P. Tomsia and R. O. Ritchie, *Science*, 2008, **322**, 1516–1520.
13 L. J. Bonderer, A. R. Studart and L. J. Gauckler, *Science*, 2008, **319**, 1069–1073.
14 A. Walther, I. Bjurhager, J. M. Malho, J. Ruokolainen, L. A. Berglund and O. Ikkala, *Angew. Chem., Int. Ed.*, 2010, **49**, 6448–6453.
15 R. M. Erb, R. Libanori, N. Rothfuchs and A. R. Studart, *Science*, 2012, **335**, 199–204.
16 G. Decher, *Science*, 1997, **277**, 1232–1237.
17 S. J. Eichhorn, A. Dufresne, M. Aranguren, N. E. Marcovich, J. R. Capadona, S. J. Rowan, C. Weder, W. Thielemans, M. Roman, S. Renneckar, W. Gindl, S. Veigel, J. Keckes, H. Yano, K. Abe, M. Nogi, A. N. Nakagaito, A. Mangalam, J. Simonsen, A. S. Benight, A. Bismarck, L. A. Berglund and T. Peijs, *J. Mater. Sci.*, 2010, **45**, 1–33.
18 Y. Habibi, L. A. Lucia and O. J. Rojas, *Chem. Rev.*, 2010, **110**, 3479.
19 D. Klemm, F. Kramer, S. Moritz, T. Lindström, M. Ankerfors, D. Gray and A. Dorris, *Angew. Chem., Int. Ed.*, 2011, **50**, 5438–5466.
20 S. Iwamoto, W. Kai, A. Isogai and T. Iwata, *Biomacromolecules*, 2009, **10**, 2571–2576.
21 M. Pääkkö, M. Ankerfors, H. Kosonen, A. Nykänen, S. Ahola, M. Österberg, J. Ruokolainen, J. Laine, P. T. Larsson, O. Ikkala and T. Lindström, *Biomacromolecules*, 2007, **8**, 1934–1941.
22 M. Henriksson, G. Henriksson, L. A. Berglund and T. Lindström, *Eur. Polym. J.*, 2007, **43**, 3434–3441.
23 T. Saito, S. Kimura, Y. Nishiyama and A. Isogai, *Biomacromolecules*, 2007, **8**, 2485–2491.
24 K. Fleming, D. G. Gray and S. Matthews, *Chem.–Eur. J.*, 2001, **7**, 1831–1835.
25 H. Yano, J. Sugiyama, A. N. Nakagaito, M. Nogi, T. Matsuura, M. Hikita and K. Handa, *Adv. Mater.*, 2005, **17**, 153–155.
26 R. Capadona, O. van den Berg, L. A. Capadona, M. Schroeter, S. J. Rowan, D. J. Tyler and C. Weder, *Nat. Nanotechnol.*, 2007, **2**, 765–769.
27 J. R. Capadona, K. Shanmuganathan, D. J. Tyler, S. J. Rowan and C. Weder, *Science*, 2008, **319**, 1370–1374.
28 L. Wågberg, G. Decher, M. Norgren, T. Lindström, M. Ankerfors and K. Axnäs, *Langmuir*, 2008, **24**, 784–795.
29 G. Siqueira, J. Bras and A. Dufresne, *Polymers*, 2010, **2**, 728–765.
30 R. T. Olsson, M. A. S. A. Samir, G. Salazar-Alvarez, L. Belova, V. Strom, L. A. Berglund, O. Ikkala, J. Nogues and U. W. Gedde, *Nat. Nanotechnol.*, 2010, **5**, 584–588.
31 C. Aulin, J. Netrval, L. Wågberg and T. Lindström, *Soft Matter*, 2010, **6**, 3298–3305.
32 P. Laaksonen, A. Walther, J. M. Malho, M. Kainlauri, O. Ikkala and M. B. Linder, *Angew. Chem., Int. Ed.*, 2011, **50**, 8688–8691.
33 H. Sehaqui, A. D. Liu, Q. Zhou and L. A. Berglund, *Biomacromolecules*, 2010, **11**, 2195–2198.
34 A. D. Liu, A. Walther, O. Ikkala, L. Belova and L. A. Berglund, *Biomacromolecules*, 2011, **12**, 633–641.
35 H. Jin, M. Kettunen, A. Laiho, H. Pynnönen, J. Paltakari, A. Marmur, O. Ikkala and R. H. A. Ras, *Langmuir*, 2011, **27**, 1930–1934.
36 J. T. Korhonen, M. Kettunen, R. H. A. Ras and O. Ikkala, *ACS Appl. Mater. Interfaces*, 2011, **3**, 1813–1816.
37 M. Wang, A. Olszewska, A. Walther, J. M. Malho, F. H. Schacher, J. Ruokolainen, M. Ankerfors, J. Laine, L. A. Berglund, M. Österberg and O. Ikkala, *Biomacromolecules*, 2011, **12**, 2074–2081.

38 H. Jin, A. Marmur, O. Ikkala and R. H. A. Ras, *Chem. Sci.*, 2012, **3**, 2526–2529.
39 C.-N. Wu, T. Saito, S. Fujisawa, H. Fukuzumi and A. Isogai, *Biomacromolecules*, 2012, **13**, 1927–1932.
40 T. T. T. Ho, Y. S. Ko, T. Zimmermann, T. Geiger and W. Caseri, *J. Mater. Sci.*, 2012, **47**, 4370–4382.
41 A. Okada and A. Usuki, *Mater. Sci. Eng., C*, 1995, **3**, 109–115.
42 E. P. Giannelis, *Adv. Mater.*, 1996, **8**, 29–35.
43 P. C. LeBaron, Z. Wang and T. J. Pinnavaia, *Appl. Clay Sci.*, 1999, **15**, 11–29.
44 Y. S. Lu and R. C. Larock, *Biomacromolecules*, 2006, **7**, 2692–2700.